Molecular Dynamics Simulations of Nuclear Pasta

A.S. Schneider[1], J. Hughto[1], C.J. Horowitz[1], D.K. Berry[2]

[1]Department of Physics and Nuclear Theory Center
Indiana University

[2]University Information Technology Center
Indiana University

East Lansing - MI - July 2013

NUCLEI
Nuclear Computational Low-Energy Initiative

Nuclear Pasta

Physics of matter at densities of about $\sim 10^{13} - 10^{14}\,\mathrm{g/cm^3}$.

- Present in core-collapse supernovae and neutron-star crusts;
- Small densities ($\rho \ll \rho_0$) $\Rightarrow$ isolated nuclei;
- Large densities ($\rho \gtrsim \rho_0$) $\Rightarrow$ uniform matter.

- In between matter is *frustrated*, *i.e.*, energy scale of nuclear forces and Coulomb forces is comparable;
- Competition between the two forces makes nucleons cluster in complex shapes.
- Our goal is to determine how during a supernovae the core of a star transforms from 10^{55} separate nuclei into a single large nucleus (neutron star).
- Use MD to simulate very large systems for very long times and calculate complex observables.

Nuclear Pasta

As density increases neutrons drift out of nuclei. Then protons drift out of nuclei.

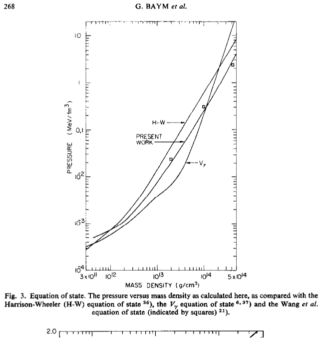

Figure: From Nuclear Physics A 175 225 (1971). Equation of State

Nuclear Pasta

Lamb *et al.*: liquid-drop model
As density increases matter turns "inside out".

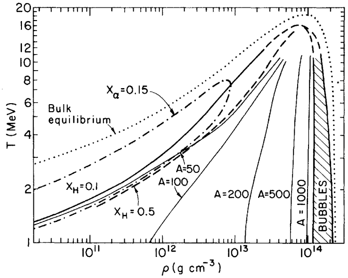

FIG. 1. Composition of hot dense matter for $Y_e = 0.25$. For comparison, the dotted curve shows the boundary of the two-phase region for bulk equilibrium.

Figure: From Phys Rev Lett 41 1623 (1978). Composition of hot dense matter.

Nuclear Pasta

Ravenhall *et al.* using a liquid-drop model suggest that "cylindrical and planar geometries can occur, both as nuclei and as bubbles".
Condition for equilibrium is that $E_{\rm sur} = 2E_{\rm c}$, regardless of dimensionality.

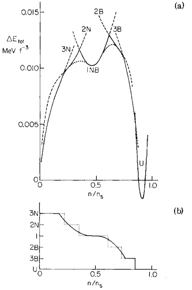

FIG. 1. (a) A plot of $E_{\rm tot}$ vs n/n_s for the five phases N, $2N$, $1NB$, $2B$, and $3B$, and the uniform matter hase. Each is shown as a dashed curve except for he region in which it is the most stable phase, where t is shown as a full curve. The dotted curves show $_{\rm tot}$ for the continuous dimensionality phase. For il- ıstrative purposes a common background function of $/n_s$ has been subtracted. (b) The continuous dimen- ionality d vs n/n_s (full curve). The dotted lines cor- espond to the energy crossings of the discrete-d

Figure: From Phys Rev Lett 50 2066 (1983). Densities for which each pasta phase occurs.

Nuclear Pasta

Hashimoto *et al.* also show that "stable nuclear shape is likely to change successively from sphere to cylinder, board, cylindrical hole and spherical hole before uniform neutron-star matter is formed."

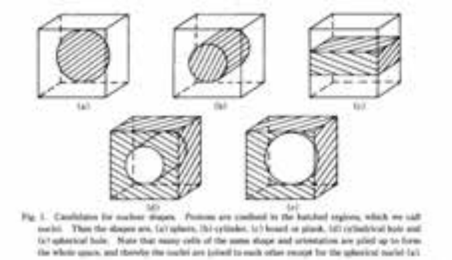

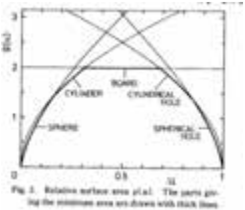

Figure: From Progress of Theoretical Physics 71 320 (1984). Pasta phases and densities which they occur.

Nuclear Pasta

Williams and Koonin used Thomas-Fermi approximation which allowed for arbitrary shapes within the unit cell.
Obtained that transitions between pasta phases are of first-order.

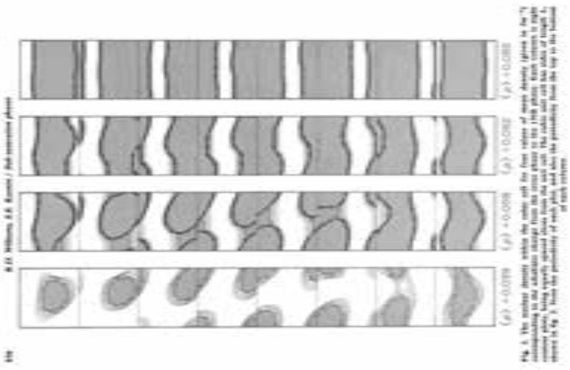

Figure: From Nuclear Physics A 435 844 (1985). Snapshots of pasta phases for symmetric nuclear matter.

Nuclear Pasta

Okamoto *et al.* Thomas-Fermi approximation

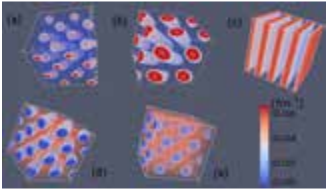

Fig. 1. (Color online.) Proton density distributions of the ground states of symmetric matter ($Y_p = 0.5$). Typical pasta phases are observed: (a) Spherical droplets with a fcc crystalline structure at baryon density $\rho_B = 0.01$ fm^{-3}. (b) Cylindrical rods with a honeycomb crystalline structure at 0.024 fm^{-3}. (c) Slabs at 0.05 fm^{-3}. (d) Cylindrical tubes with a honeycomb crystalline structure at 0.08 fm^{-3}. (e) Spherical bubbles with a fcc crystalline structure at 0.09 fm^{-3}.

Fig. 8. Proton density distributions with complex structures ($Y_p = 0.5$). (a) Mixture of droplet and rod, 0.022 fm^{-3}; (b) slab and tube, 0.068 fm^{-3}; (c) dumbbell like structure, 0.018 fm^{-3}; (d) diamond like structure, 0.048 fm^{-3}.

Figure: From Physics Letters B 713 284 (2012). Snapshots of pasta phases for symmetric nuclear matter.

Nuclear Pasta

W. Newton and J.R. Stone Skyrme-Hartree-Fock + BCS

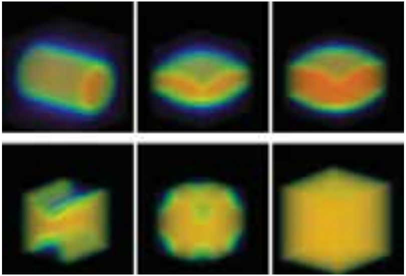

FIG. 11. (Color online) 3D renderings of the neutron density prof les of minimum energy conf gurations at $T = 2.5$ MeV and densities of $n_b = 0.04$ fm^{-3} (top left), $n_b = 0.06$ fm^{-3} (top middle), $n_b = 0.08$ fm^{-3} (top right), $n_b = 0.09$ fm^{-3} (bottom left), $n_b = 0.10$ fm^{-3} (bottom middle), and $n_b = 0.11$ fm^{-3} (bottom right). Dark (blue) colors, mostly along the surface regions indicate the lowest densities and gray (red) the highest, traversing the volume (see color online version for clarity).

Figure: From Physical Review C 79 055801 (2009). Snapshots of pasta phases for nuclear matter with proton fraction of 0.30.

Nuclear Pasta

Watanabe *et al.* QMD

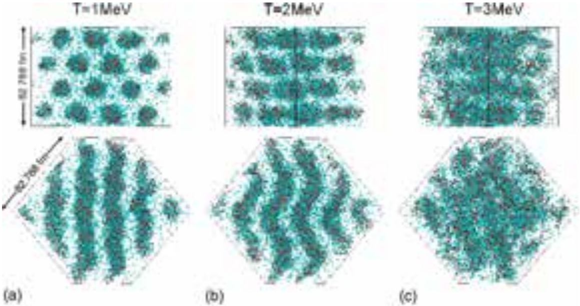

FIG. 8. (Color online) The nucleon distributions for x=0.3, =0.175 $_0$ at the temperatures of 1, 2, and 3 MeV. 16384 nucleons are contained in the simulation box of size L_{box}=82.788 fm. Protons are represented by the red particles, and neutrons by the green ones. The upper panels show the top views along the axis of the cylindrical nuclei at T=0, and the lower ones show the side views.

Figure: From Physical Review C 69 055805 (2004). Snapshots of pasta phases for nuclear matter with proton fraction of 0.30.

Nuclear Pasta

Nakazato *et al.* Liquid-drop model

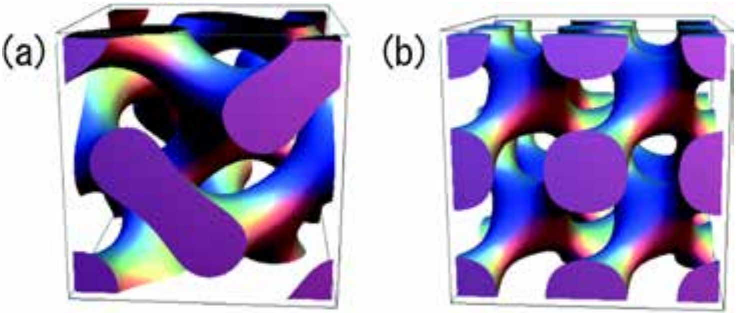

FIG. 1 (color online). Bird's-eye views of unit cubes of (a) gyroid and (b) double-diamond, in which bicontinuous minimum surfaces are shown for volume fraction u ¼ 0:35.

Figure: From Physical Review Letters 103 132501 (2009). Snapshots of pasta phases for nuclear matter with proton fraction of 0.30.

Nuclear Pasta

H. Pais and J.R. Stone Skyrme-Hartree-Fock + BCS

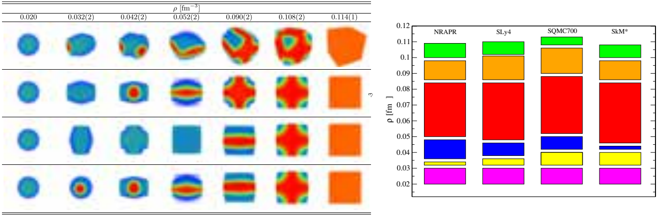

Figure: From Physical Review Letters 109 151101 (2012). Snapshots of pasta phases for nuclear matter with proton fraction of 0.30. Pasta phases: spherical bubbles (magenta), rod (yellow), cross rods (blue), slabs (yellow), cylindrical holes (orange), spherical holes (green).

Nuclear Pasta

Schuetrumpf *et al.* Time-dependent Hartree-Fock

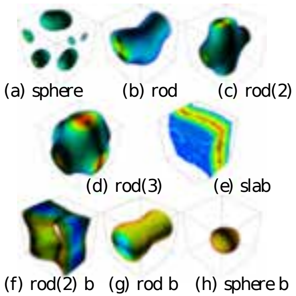

Figure 1. Typical pasta shapes at T = 7 MeV. Bubble shape illustrations show gas phase indicated by the color-scale.

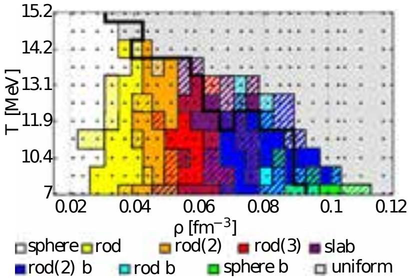

Figure 2.

Figure: From Journal of Physics: Conference Series 426 012009 (2012). Snapshots of pasta phases for nuclear matter with proton fraction of $1/3$.

Maximum Pasta Density

- RPA stability analysis of nuclear matter finds density where uniform system first becomes unstable to density fluctuations.
- Good approximation to crust core transition density.

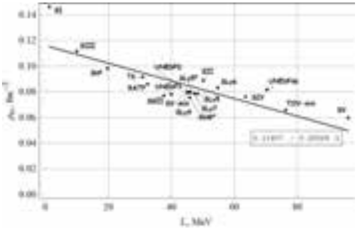

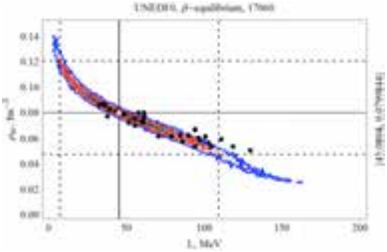

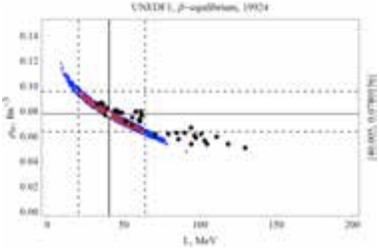

Sergey Postnikov

Minimum Pasta Density

- Pasta occurs when nuclei become unstable to fission.
- If $E_{\mathrm{sur}} > E_{\mathrm{c}}$ then spherical nuclei can undergo large deformations.
- If minimum density > maximum density pasta will not form.

Formalism

Classical system of protons and neutrons immersed in a background electron gas.

Nucleons interact through a potential:

$$V_{ij}(r_{ij}) = a e^{-r_{ij}^2/\Lambda} + [b + c\tau_z(i)\tau_z(j)] e^{-r_{ij}^2/2\Lambda} + V_{ij}^C(r_{ij})$$

where

$$V_{ij}^C(r_{ij}) = \frac{e^2}{r_{ij}} e^{-r_{ij}/\lambda} \tau_p(i)\tau_p(j), \qquad \tau_p \equiv (1+\tau_z)/2$$

and $\lambda = \frac{\pi^{1/2}}{2e}\left(k_F\sqrt{k_F^2 + m_e^2}\right)^{-1/2}$ is the Thomas-Fermi screening length for relativistic electrons, $k_F = (3\pi^2 n_e)^{1/3}$ is the Fermi momentum and n_e the e^- density.

Formalism

a	b	c	Λ	λ^*
110 MeV	-26 MeV	24 MeV	1.25 fm^2	10 fm

Table: Model parameters used in the calculations. λ was arbitrarily decreased to 10 fm.

Reasonable results for binding energies of finite nuclei.

Nucleus	Monte-Carlo $\langle V_{tot} \rangle$ (MeV)	Experiment (MeV)
^{16}O	-7.56±0.01	-7.98
^{40}Ca	-8.75±0.03	-8.45
^{90}Zr	-9.13±0.03	-8.66
^{208}Pb	-8.2 ± 0.1	-8.45

Table: Binding energies per nucleon in MeV from parameters defined above from Phys Rev C 69 405804

Formalism

- Neutron matter is unbound;
- Reasonable results for energy per nucleon for symmetric nuclear matter;
- Saturates in the correct density;

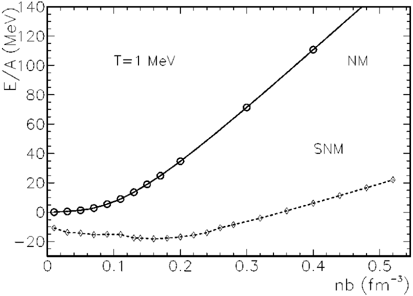

Figure: Energy per nucleon for symmetric (dashed) and pure-neutron (solid) matter *vs* baryon density *nb* at $T = 1\,\mathrm{MeV}$. From Phys Rev C 69 405804.

Simulations

- Number of particles $N = 51\,200$;
- Proton fraction $Y_p = 0.40$: $30\,720$ neutrons and $20\,480$ protons;
- Temperature of $1\,\mathrm{MeV}$ (approximate infall phase of a SN);
- Cubic box with periodic boundary conditions;
- Start from random at a density of $0.10\,\mathrm{fm}^{-3}$ (box side is $80\,\mathrm{fm}$);
- Expand the system at different rates $\dot{\xi}$;
- After expansion starts, side of the box at time t:

$$l(t) = l_0(1 + \dot{\xi} t);$$

- Compare topology the systems stretched at different rates.

Simulations

Visualization of system with $Y_p = 0.40$ at $T = 1\,\mathrm{MeV}$ stretch at a rate of $\dot{\xi} = 2.0 \times 10^{-8}\mathrm{c/fm}$. Animation generated with ParaView 3.98.

Simulations

Code

- Fortran 95 code.
- Optimized to run on supercomputers with hybrid architecture.
- Use Kraken supercomputer.
    - Machine with 9408 nodes.
    - Each node has 2 processors.
    - Each processor has 6 cores.

Usage

- MPI for each processor on a node;
- OpenMP for each core;
- This simulation: 144 nodes $\Rightarrow$ 864 cores.
- 600 hours (25 days) of simulation time.

Topological Characterization

Minkowski functionals

- $W_1 \propto V$ — Volume V;
- $W_2 \propto \int_{\partial K} dA$ — Surface area A;
- $W_3 \propto \int_{\partial K} \left(\frac{\kappa_1+\kappa_2}{2}\right) dA$ — Mean breadth B;
- $W_4 \propto \int_{\partial K} (\kappa_1 \cdot \kappa_2)\, dA$ — Euler characteristic χ.

κ_1 and κ_2 are the principal curvatures on ∂K the bounding surface of K.

$\chi =$ (# isolated regions) - (# tunnels) + (# cavities)

Use B/A and χ/A as measures to compare systems.

Curvature

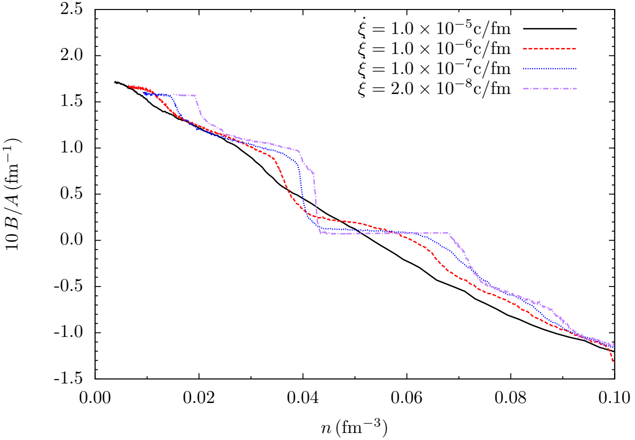

Figure: Normalized mean breadth B/A as a function of density n for different stretch rates. The simulations contain 51 200 nucleons with $Y_p = 0.40$ at $1\,\mathrm{MeV}$.

Curvature

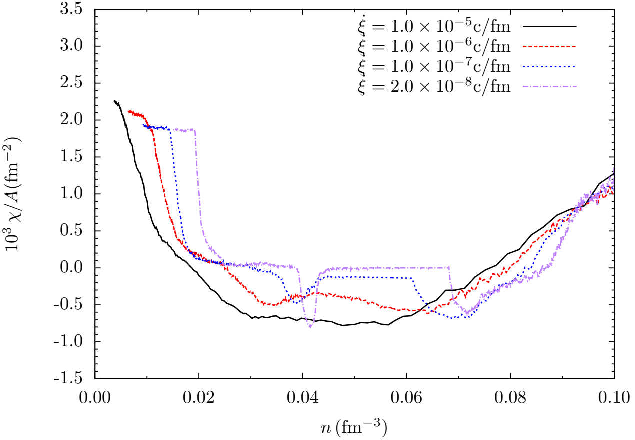

Figure: Normalized Euler characteristic χ/A as a function of density n for different stretch rates. The simulations contain 51 200 nucleons with $Y_p = 0.40$ at $1\,\mathrm{MeV}$.

Curvature

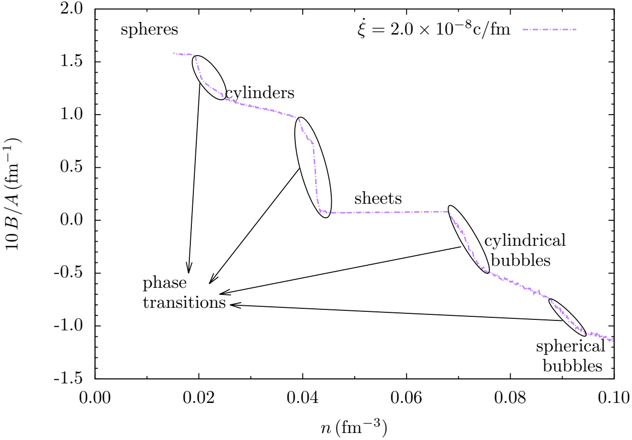

Figure: Normalized mean breadth B/A as a function of density n for for $\dot{\xi} = 2.0 \times 10^{-8}\,\mathrm{c/fm}$. The simulations contain 51 200 nucleons with $Y_p = 0.40$ at $1\,\mathrm{MeV}$.

Curvature

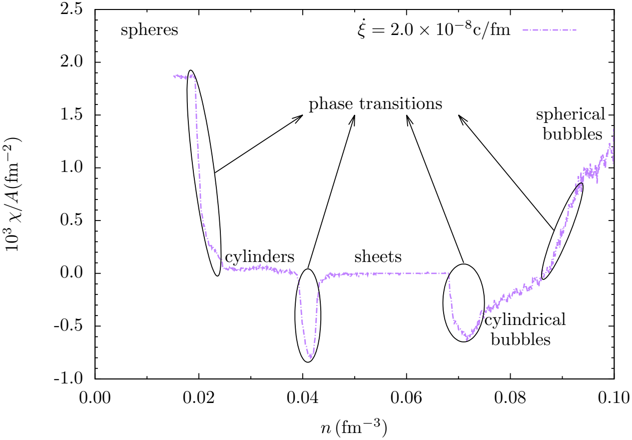

Figure: Normalized Euler characteristic χ/A as a function of density n for $\dot{\xi} = 2.0 \times 10^{-8}\,\mathrm{c/fm}$. The simulations contain 51 200 nucleons with $Y_p = 0.40$ at $1\,\mathrm{MeV}$.

Transitions

Competition between Coulomb and Surface energies is responsible for phase transitions.

Figure: Phase transition from “lasagna” to “spaghetti” phase.

Transitions

Competition between Coulomb and Surface energies is responsible for phase transitions.

Figure: Phase transition from "spaghetti" to "gnocchi" phase.

Transitions

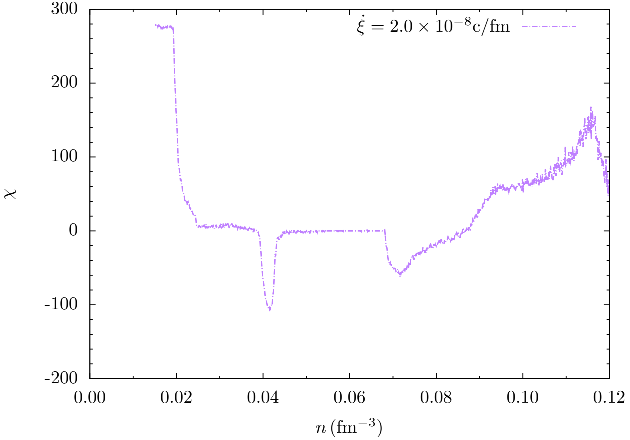

Figure: Euler characteristic χ as a function of density n for $\dot{\xi} = 2.0 \times 10^{-8}\,\mathrm{c/fm}$. The simulations contain 51 200 nucleons with $Y_p = 0.40$ at $1\,\mathrm{MeV}$.

Transitions

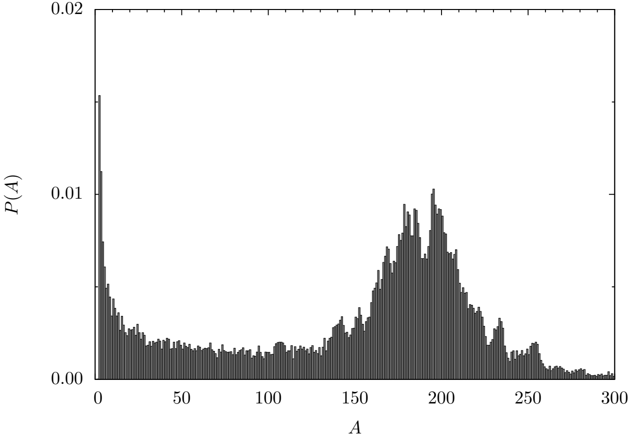

Figure: Histogram of nuclei present after transition to "gnocchi" phase for systems stretched at $\dot{\xi} = 1.0 \times 10^{-6}\,\mathrm{c/fm}$. The simulations contain 51 200 nucleons with $Y_p = 0.40$ at $1\,\mathrm{MeV}$.

Transitions

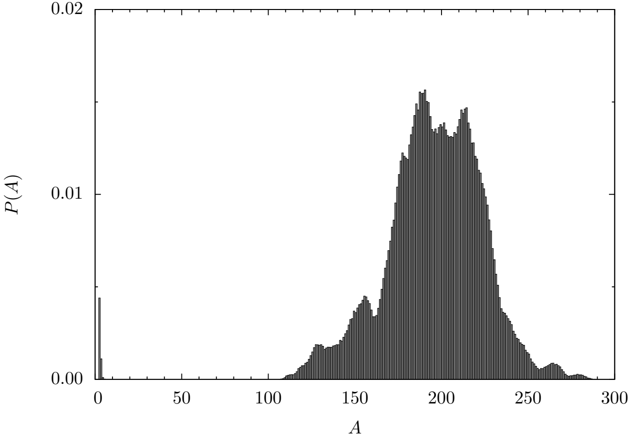

Figure: Histogram of nuclei present after transition to "gnocchi" phase for systems stretched at $\dot{\xi} = 1.0 \times 10^{-7}\,\mathrm{c/fm}$. The simulations contain 51 200 nucleons with $Y_p = 0.40$ at $1\,\mathrm{MeV}$.

Transitions

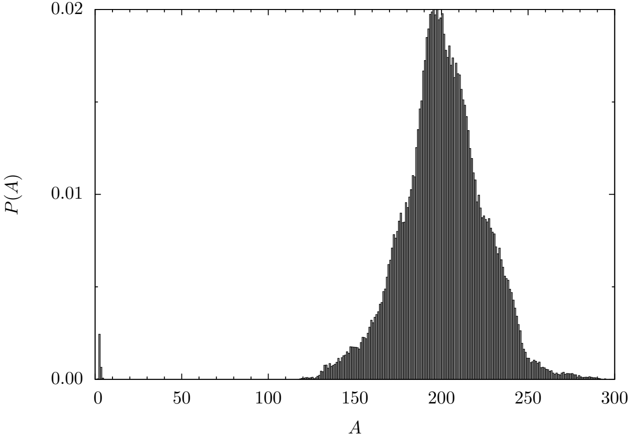

Figure: Histogram of nuclei present after transition to “gnocchi” phase for systems stretched at $\dot{\xi} = 2.0 \times 10^{-8}\,\mathrm{c/fm}$. The simulations contain 51 200 nucleons with $Y_p = 0.40$ at $1\,\mathrm{MeV}$.

Observables

Jose Pons *et al.* Nature Physics, 9, 431-434 (2013)

The lack of X-ray pulsars with spin periods > 12 s raises the question about where the population of evolved high magnetic field neutron stars has gone. Unlike canonical radio-pulsars, X-ray pulsars are not subject to physical limits to the emission mechanism nor observational biases against the detection of sources with longer periods. Here we show that a highly resistive layer in the innermost part of the crust of neutron stars naturally limits the spin period to a maximum value of about $10 - 20$ s. This high resistivity is one of the expected properties of the nuclear pasta phase, a proposed state of matter having nucleons arranged in a variety of complex shapes. Our findings suggest that the maximum period of isolated X-ray pulsars can be the first observational evidence of the existence of such phase, which properties can be constrained by future X-ray timing missions combined with more detailed models.

Observables

- **ν-oppacity**
  - Depends on coherent ν-pasta scattering.
  - Important for SN simulations as $\lambda_\nu \sim$ pasta sizes.
- **Shear viscosity**, **thermal conductivity** and **electrical conductivity**.
  - Depends on coherent e^--pasta scattering.
  - Important for NS crust properties.
- **Bulk viscosity**
  - Depends on hysteresis in pasta shapes with density changes.
  - May be important for damping of NS r-mode oscillations.
- **Shear modulus**
  - Response to small deformations of simulation volume.
  - Determines NS oscillation frequencies.
- **Breaking strain**
  - Response to large deformations of simulation volume.
  - Important for star quakes, magnetar giant flares and mountain heights.

Observables

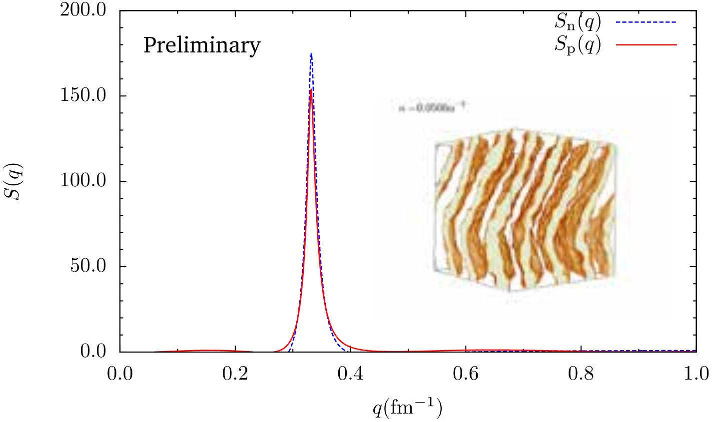

Figure: Static Structure factor for pasta configuration at $n = 0.050\,\mathrm{fm}^{-3}$.

Summary

- Perfomed large MD simulations of matter near saturation density.
- Able to describe dynamics of pasta phases and phase-transitions.
- Formalism that describes the topology of the pasta.
- Determine time-scales of phase-transitions.

Prospects

Near future:

- Find a condition for which pasta simulation has equilibrated.
- Bring finite size effects under control.
- Explore parameter space using other proton fractions and temperatures.
- Use actual Coulomb screening length.
- Obtain static structure factors of pasta phases.
- Obtain shear viscosity and bulk viscosity of different pasta structures.
- Obtain shear modulus and breaking strain of pasta.

Not so near future:

- Add other parameters to effective potential:
    - Momentum and spin dependence.